Journal of Thermal Analysis and Calorimetry, Vol. 79 (2005) 401–406

SYNTHESIS OF $Ca_xSr_{1-x}WO_4$ BY THE POLYMERIC PRECURSOR METHOD

S. L. Porto[1], *M. R. Cassia-Santos*[1], *Iêda. M. G. Santos*[1], *S. J. G. Lima*[2], *L. E. B. Soledade*[1], *A. G. Souza*[1*], *C. A. Paskocimas*[3] *and E. Longo*[4]

[1]LTM, Departamento de Química, CCEN, Universidade Federal da Paraíba, 58.059-900 João Pessoa, PB, Brazil
[2]Departamento de Engenharia Mecânica, CT, Universidade Federal da Paraíba, 58.059-900 João Pessoa, PB, Brazil
[3]Departamento de Engenharia Mecânica, CT, Universidade Federal do Rio Grande do Norte, 59.072-970 Natal, RN, Brazil
[4]CMDMC, Departamento de Química, Universidade Federal de São Carlos, São Carlos, SP, Brazil

In the present study, powders based on $Ca_xSr_{1-x}WO_4$ tungstates, with a scheelite structure were synthesized, using the polymeric precursor method. The powder precursors, calcined at 300°C, were thermally characterized by TG/DTA. It can be observed that the mass loss basically takes place in three stages: first – dehydration, second – pyrolysis and third – elimination of the remaining organic material. The structural characterization was performed by XRD, after thermal treatment between 300 and 700°C. The crystallization takes place at 500°C, but more defined and intense diffraction peaks appeared at 700°C. Based on these XRD results the lattice parameters, crystallinity and crystallite size were calculated.

Keywords: *polymeric precursor method, scheelite, tungstates*

Introduction

MWO_4 tungstates (*M*=bivalent cations) are compounds found frequently in nature, which crystallize in alkaline solutions, obtained by the melting of the binary oxide components. Similar case is known for calcium tungstate.

The tungstates can be obtained in two isostructural groups: scheelite, $CaWO_4$ and wolframite, $FeWO_4$ and $MnWO_4$. The structure will depend on the ionic radius of A^{2+} cations. For A^{2+} cations with covalent character (such as Mg^{2+} and 3d orbital ions), the wolframite structure is favored. Since Ca^{2+}, Sr^{2+} and Ba^{2+} cations have a stronger ionic character, the scheelite structure is more favorable. The transition from the scheelite structure to the wolframite one can be stimulated by high pressures – around 5 GPa for $BaWO_4$ and about 1.2 GPa for $CaWO_4$ [1]. The crystalline structure of scheelite is highly ionic, containing A^{2+} cations and WO_4^{2-} anions. Such structure presents the $I4_1/a$ or C_{4h}^6 space group in which A cations have an octahedral coordination, W cations are tetrahedrally coordinated and each unit cell has two AWO_4 units [2–5].

In recent years, the scheelite structure reached remarkable attention due to its attractive electro-optical properties. Blasse *et al*. [6] investigated the luminescence of barium and strontium tungstate synthesized by solid-state reactions. They obtained a system with scheelite structure, displaying luminescent properties (which varied with the concentration of these metals). They observed a green and blue emission for some samples excited in the short ultraviolet wavelength at cryogenic temperatures ($N_2(l)$ for $SrWO_4$ and $H_2(l)$ for $BaWO_4$). The blue emission was only observed for the samples calcined at a low temperature. Therefore, the study of the thermal and structural properties of tungstate-based systems becomes more and more important and necessary investigate their optical properties.

This is the reason, why in the present work, the synthesis of ceramic tungstates with molecular formula of $Ca_xSr_{1-x}WO_4$ (with x=0, 0.2, 0.4, 0.6, 0.8 and 1.0) with scheelite structure was carried out. The synthesis has been carried out by the 'Pechini' method [7]. The method was selected because of its efficiency, presenting some peculiar characteristics, such as a good homogeneity at the atomic level.

Experimental

Powder synthesis

All the tungstate-based powders were prepared keeping the following stages: 1) preparation of tungsten citrate; 2) Synthesis of the polymeric resin; 3) first calcination, obtaining of the precursor powder; 4) second calcination, obtaining samples with different crystallinity degrees.

Tungsten citrate was chosen as cationic precursor in the preparation of the precursor resins for the synthesis of the compounds displaying the molecular formula $Ca_xSr_{1-x}WO_4$ (x=0.0, 0.2, 0.4, 0.6, 0.8 and 1.0).

* Author for correspondence: agouveia@quimica.ufpb.br

1388–6150/$20.00

Akadémiai Kiadó, Budapest, Hungary
Springer, Dordrecht, The Netherlands

This citrate was obtained by dissolving tungstic acid in a citric acid solution, under constant agitation at 70°C. Ammonium hydroxide was slowly added to this aqueous solution in order to provide the complete dissolution of the tungstic acid at pH≈8. After some hours of continuous agitation, a limpid and transparent tungsten citrate was obtained.

After the synthesis of this citrate, the $SrCO_3$ and $CaCO_3$ salts were slowly added to the citrate, till their total dissolution. 3:1 citric acid:metal cation molar ratio was used in order to guarantee the complete metal chelation. Then ethylene glycol was added to the solution. 40:60 citric acid:ethylene glycol mass ratio was used. The reaction temperature was raised to approximately 90°C to promote the esterification and the evaporation of the water excess. Limpid solutions were obtained, which were heated to 300°C, at air resulting a semi-carbonized material displaying a foam-type structure, called to powder precursor. These precursors were de-agglomerated in a porcelain mortar and were ground until passing through a 200 mesh-sieve. The thermal characterization of these precursors was performed by thermogravimetry (TG) and differential thermal analysis (DTA).

The powder precursors were calcined, at air atmosphere at 300°C for 2 h and then at 400, 500, 600 and 700°C for 4 h, at a heating rate of 5 K min^{-1}.

Powder characterization

The thermal characterization of the powder precursors was done by TG/DTA. In the TG experiments, a Shimadzu model TGA-50 thermobalance was used, with air atmosphere (flow rate of 30 mL min^{-1}) heating rate: 10 K min^{-1} between 30 and 900°C the initial sample mass was about 10 mg. For DTA measurements, a TA Instruments equipment was used, with a synthetic air (flow rate of 30 mL min^{-1}) and under the above written conditions.

The formation of the crystalline phase as a function of the temperature and the amount of added calcium was followed by X-ray diffraction (XRD), using a D 5000/Siemens diffractometer.

Results and discussion

The TG/DTG curves representing the thermal behavior of $Ca_xSr_{1-x}WO_4$ ($0 \le x \le 1$) powder precursors are presented in Fig. 1. Basically, the mass losses appear in three stages: 1) up to 300°C, which is attributed to water elimination, corresponding to the partial dehydration of the compounds; 2) from 270 up to 620°C, two consecutive processes occur, corresponding to the polymer degradation, with the elimination of CO_2 and

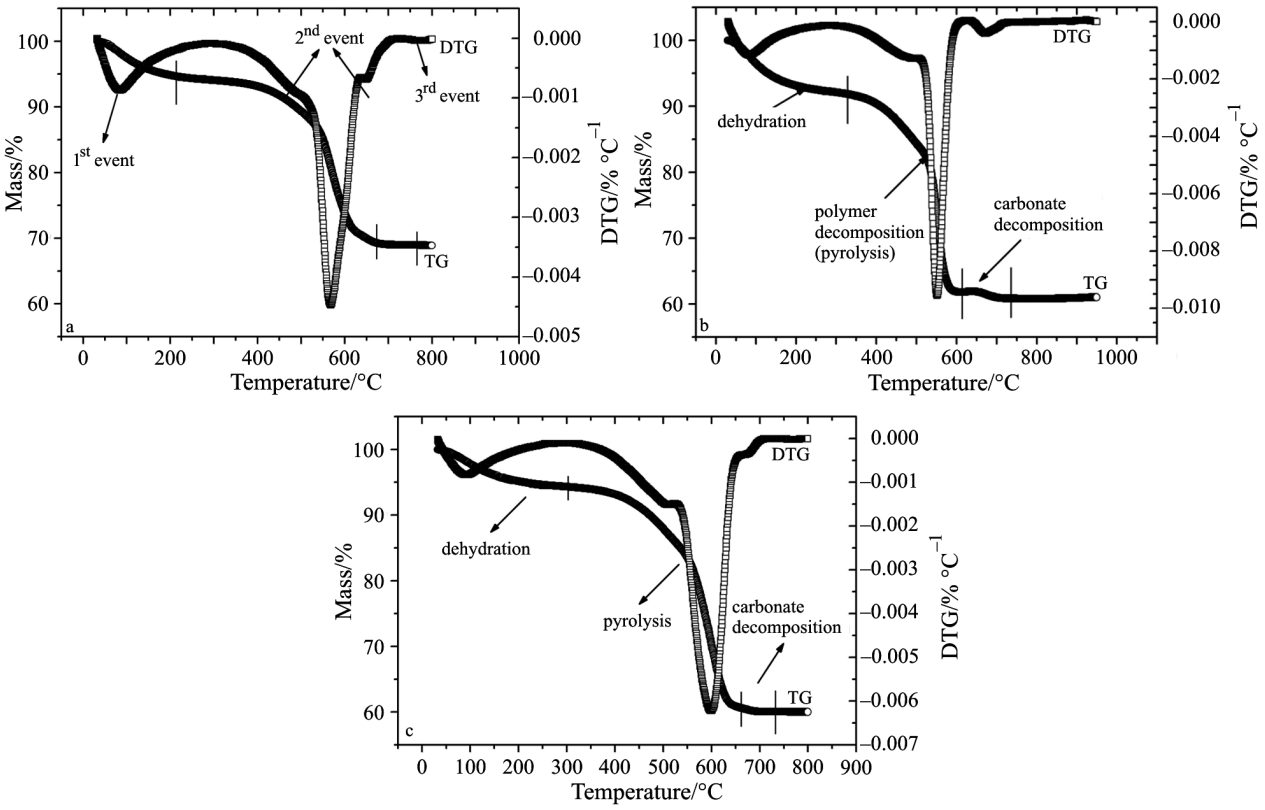

Fig. 1 TG/DTG curves of the $Ca_xSr_{1-x}WO_4$ powder precursor system; a – x=0.0, b – x=1.0, c – x=0.8

H_2O, and the loss of the remaining organic material, respectively; 3) between 620 and 720°C the small mass loss observed may representative for the decomposition of the carbonate formed during the pyrolysis of the material, as it will be shown by DTA [8, 9].

The DTA curves of the same three compounds are presented in Fig. 2. Exotherm and endotherm transitions can be observed for all samples. The first exotherm peak is attributed to the polymer combustion. This stage was supported by the TG curves, indicating a mass loss at about 550°C. The second endotherm peak is associated to the carbonate decomposition, possibly formed during the second event – the polymer pyrolysis. Small endotherm peaks due to dehydration are observed only for samples containing Ca and Sr, which present a higher mass loss at low temperatures.

The diffraction patterns of the $Ca_xSr_{1-x}WO_4$ system are presented in Fig. 3. After calcination at 400°C, a diffuse band is observed, indicating the predominance of the amorphous phase. After calcination at 500°C the diffraction peaks related to the crystalline phase are observed. Nevertheless, these peaks are still wide, showing that a major part of the material is still amorphous. The increase of the calcination temperature to 600°C increases the crystallinity of the sample, showing a better defined diffraction peaks, evidenced by the decrease of the full width at half maximum values of the peaks. After calcination at 700°C, the formation of a crystalline phase is observed, resulting even more defined diffraction peaks compared to the ones observed after calcination at 600°C.

As carbon loss starts at about 270°C, there is enough time for its elimination followed by sample crystallization.

All the diffraction peaks were indexed as representatives of the tetragonal scheelite unit cell. At 500°C the samples already display a scheelite phase and the increase of the calcination temperature favors the organization of this structure, eliminating structural defects, as a consequence of atomic movement by a solid-state diffusion process (Fig. 3). These results suggest the formation of a single-phase substitutional solid solution. This behavior was expected as the system satisfies the three basic conditions for substitutional solid solution formation: the Ca^{2+} ionic radius (1.12 Å) is 11.6% smaller than the ionic radius of Sr^{2+} (1.25 Å); the crystalline structures of $CaWO_4$ and $SrWO_4$ are the same; and the electropositive characters of the two cations are similar.

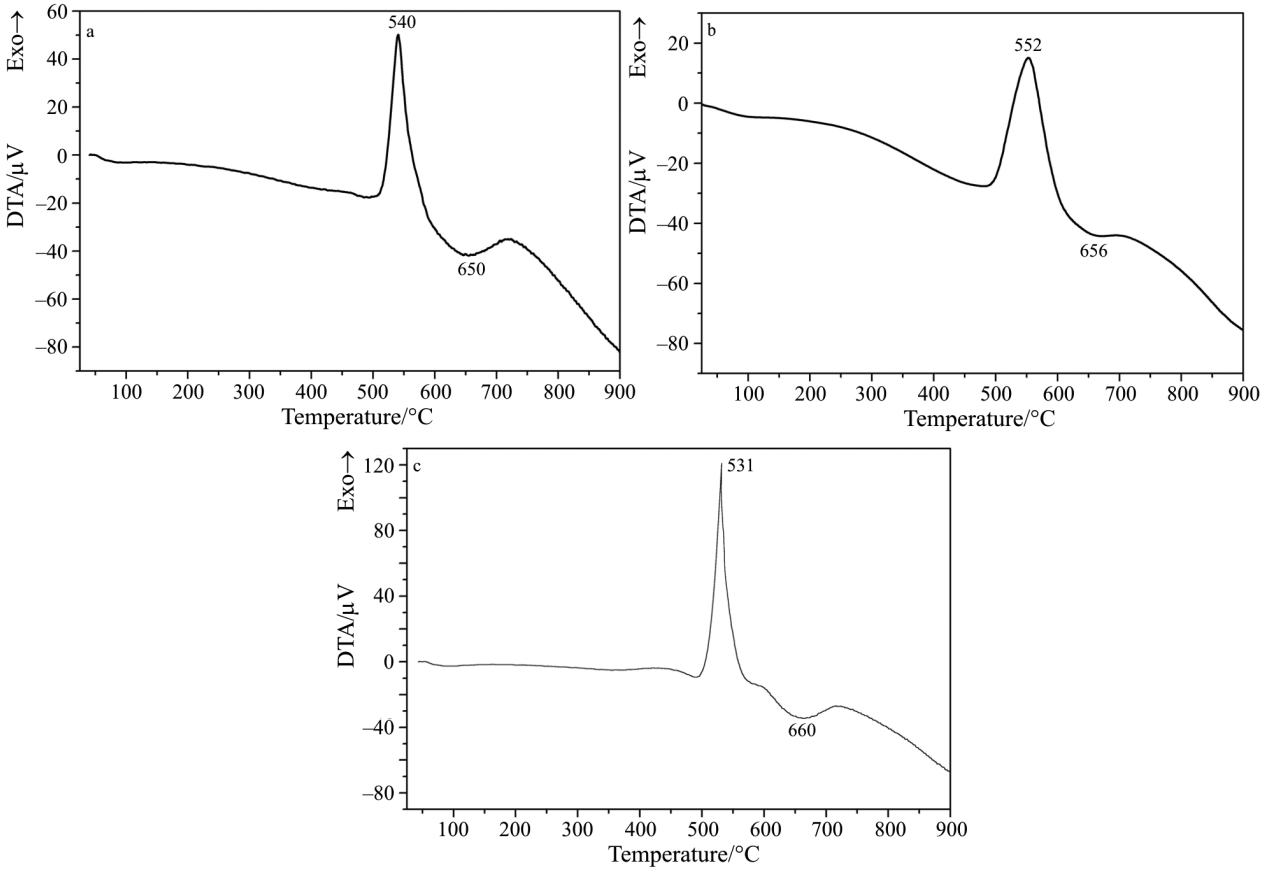

Fig. 2 DTA curves of the $Ca_xSr_{1-x}WO_4$ powder precursor system; a – x=0.0, b – x=1.0, c – x=0.8

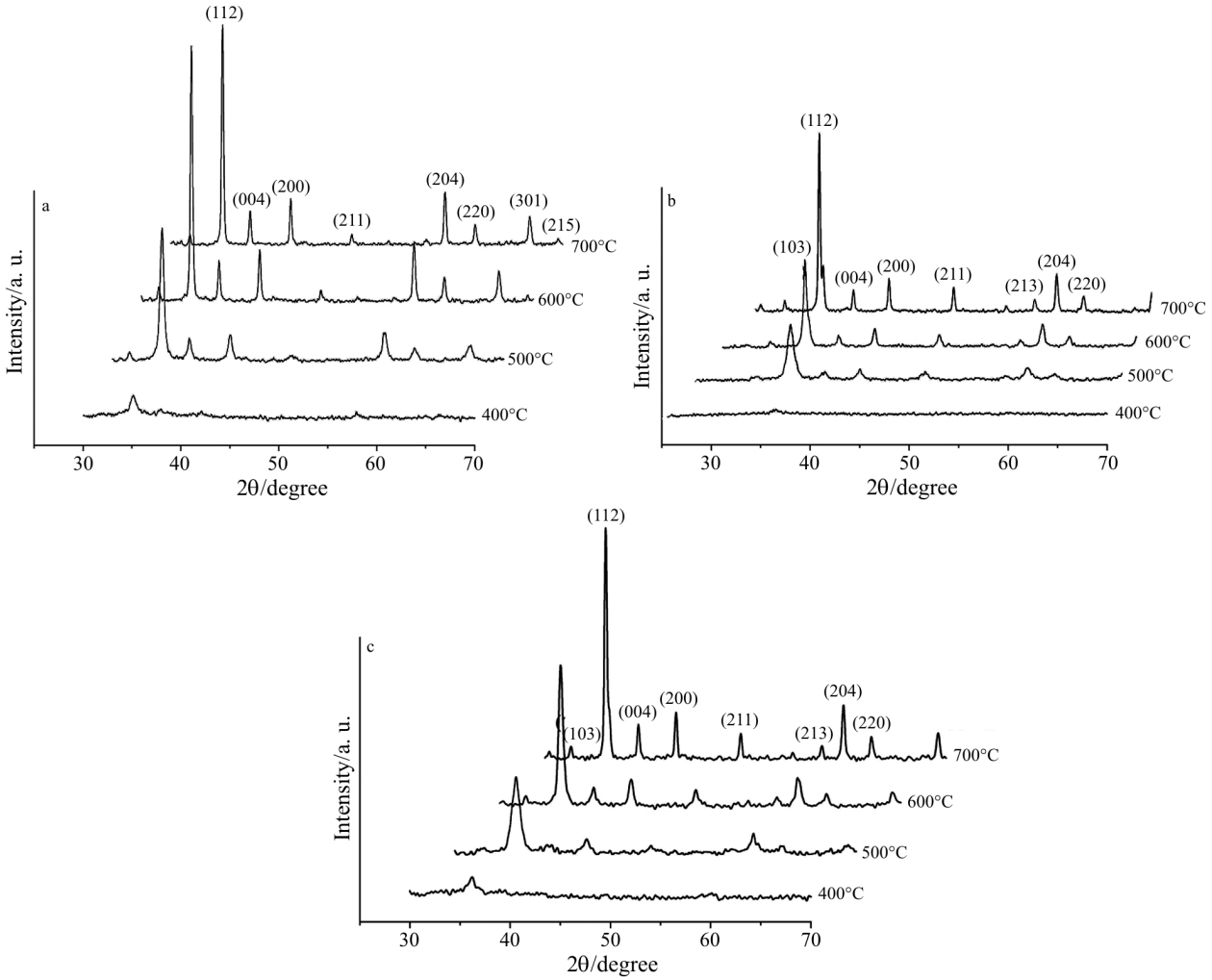

Fig. 3 X-ray diffraction patterns of the $Ca_xSr_{1-x}WO_4$ system as a function of calcination temperature; a – x=0.0, b – x=1.0, c – x=0.8

Comparing the diffractograms of Fig. 3, it is observed that the strontium tungstate ($SrWO_4$) also presents a band after calcination at 400°C. At 500°C, $SrWO_4$ presents higher diffraction peaks than $CaWO_4$, indicating that it crystallizes at a lower temperature. This evidences that in the presence of calcium the crystallization process more hindered.

With the data obtained by XRD and using the Rede 93 program, it was possible to determine the lattice parameters a and c of the system $Ca_xSr_{1-x}WO_4$ ($0 \leq x \leq 1$), as a function of calcination temperature (Fig. 4). The calcium addition led to a decrease in the lattice parameters (a and c), and consequently a reduction in the unit cell volume of the $SrWO_4$ lattice. This result is attributed to the difference in the ionic radii of the cations. The replacement of the bigger Sr^{2+} cation, (ionic radius of 1.25 Å) by a smaller Ca^{2+} cation (ionic radius of 1.12 Å) results the shrinkage of the unit cell. The experimental values of the parameters a and c, and of the unit cell volume (V) obtained in the present work are very close to the values reported in the JCPDS index card for $CaWO_4$ (JCPDS 41-1431: a=5.24294 Å, c=11.373 Å and V=312.63 Å^3) and for $SrWO_4$ (JCPDS 8-490: a=5.4168 Å, c=11.951 Å and V=350.66 Å^3).

The unit cell microstrain can be evaluated on the base of full width at half maximum values (FWHM) of the most intense peak (112), Fig. 4d. The peak is getting narrower (112) as the calcination temperature is increased. This behavior indicates a reciprocal relationship between temperature and the microstrain of the crystalline structure. The influence of the network modifier on the $MeWO_4$ structure was also observed. Calcium and strontium act as modifiers, promoting or increasing the formation of non bridging oxygens (NBO) within the three-dimensional lattice, generating structural defects, which favors the system disorder and consequently, the microstrain. The presence of calcium concomitant and strontium in the lattice increases the disorder, comparing to undoped $SrWO_4$ and $CaWO_4$. After calcination at 500 and 600°C, strontium tungstate

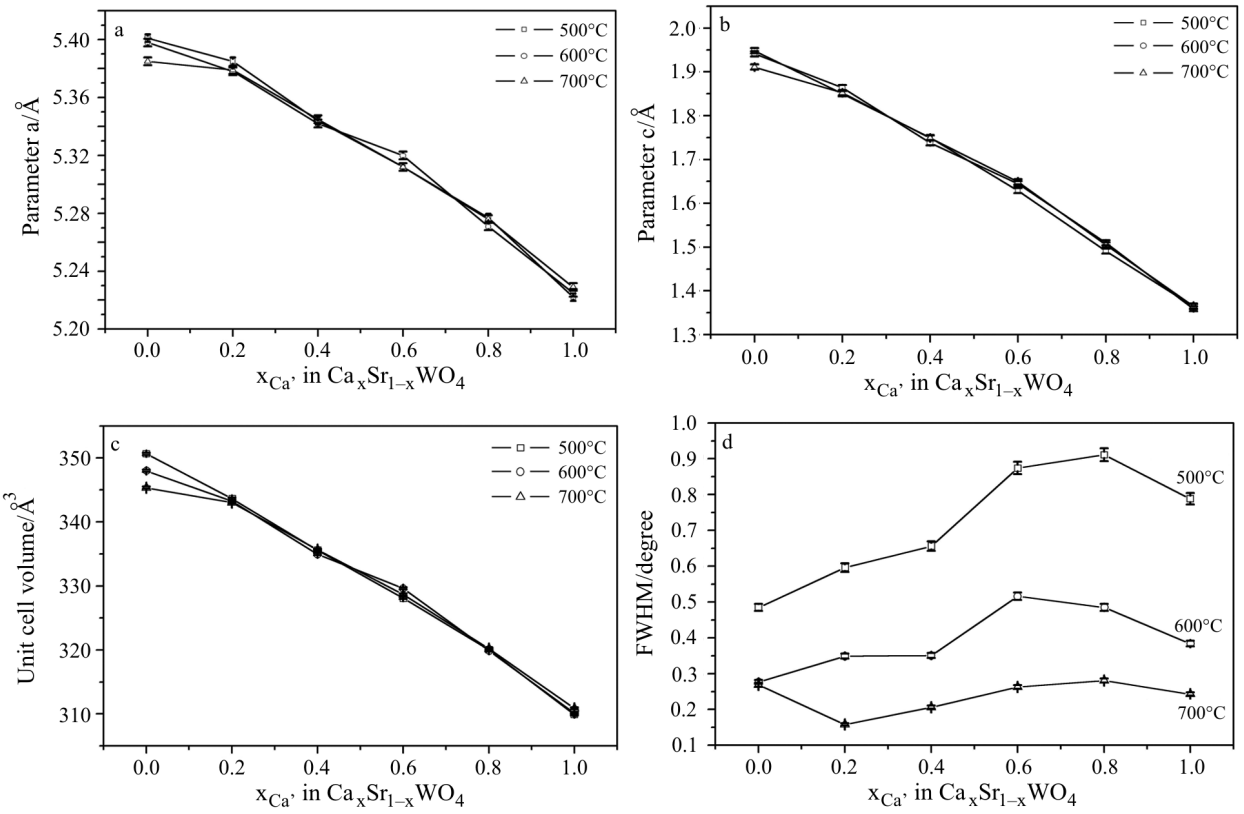

Fig. 4 Structural parameters calculated from the X-ray diffraction data for the $Ca_xSr_{1-x}WO_4$ system as a function of x at different calcination temperatures: a – lattice parameter a, b – lattice parameter c, c – unit cell volume, d – full width at half maximum (FWHM) of the 100% peak

presents a lower degree of microstrain than the calcium tungstate but at 700°C the degrees of microstrain are much closer, as it is indicated in Fig. 4.

Relative crystallinity was calculated using the 100% peak intensities and Eq. (1).

$$CR(\%) = \frac{I - I_0}{I_{100} - I_0} \cdot 100 \qquad (1)$$

where I=intensity of the (110) plane peak; I_0=intensity of the (110) plane peak of the less crystalline sample; I_{100}=intensity of (110) plane peak of the most crystalline sample.

Relative crystallinity of samples of the $Ca_xSr_{1-x}WO_4$ system for different (x) values and different calcination temperatures are presented in Fig. 5a. It can be observed that the increase in the temperature favors the crystallization, except for $SrWO_4$ calcined at 600°C. It could be observed that undoped $SrWO_4$ crystallizes at lower temperature than $CaWO_4$ under the same conditions. The increase of crystallinity was ascribed to the incorporation of the atoms in the lattice which is a thermally activated process and originates from the atomic movement by diffusion. Undoped $SrWO_4$ and $CaWO_4$ present a higher relative crystallinity than the samples containing both modifiers, showing their influence in the nucleation and crystal growing. It is also observed that the relative crystallinity decreases up to 60 mol% of calcium, and for higher amounts of Ca the relative crystallinity increases again.

This finding can be attributed to the presence of the two different network modifiers (Ca and Sr), with different ionic radii, favoring the lattice disorder. This behavior is compatible with FWHM results, which indicate a higher microstrain for samples containing both modifiers.

In Fig. 5b, the results of the crystallite sizes as a function of the calcium content and of the calcination temperature are presented. It can be observed the higher the calcination temperature, the larger the crystallite size. This effect is attributed to the phenomena of nucleation and grain growth which is a thermally activated process. From the crystallite size values, it is also verified that the increase of the calcium concentration in the $Ca_xSr_{1-x}WO_4$ system promotes a decrease of the crystallite size up to the molar percentage of 60%. For a higher calcium content, an increase of the crystallite size is observed, which can be better visualized at 700°C. This result is in agreement with the previous findings.

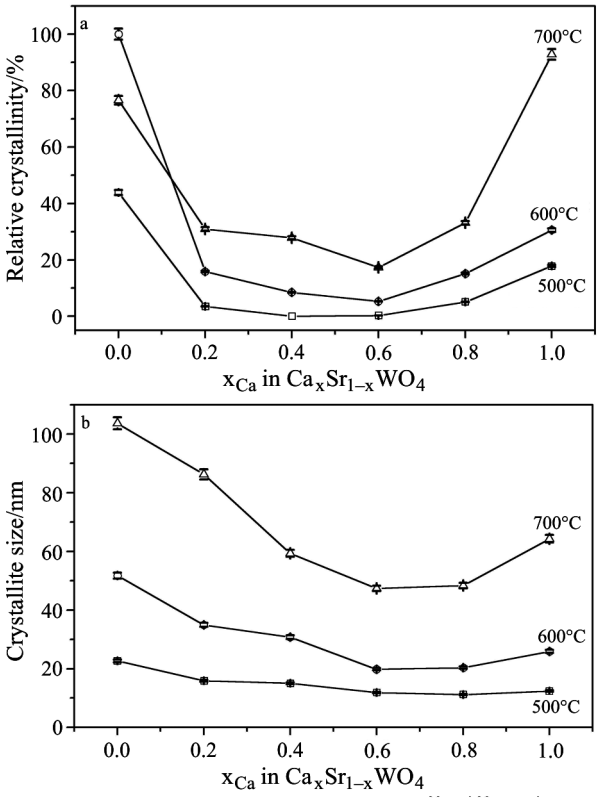

Fig. 5 a – Relative crystallinity and b – crystallite size of the $Ca_xSr_{1-x}WO_4$ system as a function of *x* at different calcination temperatures

All these results clearly show the influence of calcium on the microstructural characteristics of the system $Ca_xSr_{1-x}WO_4$.

Conclusions

Polymeric precursor method was used in the synthesis of the $Ca_xSr_{1-x}WO_4$ ($0 \leq x \leq 1$) system and resulted single-phase powders at relatively low temperatures. Their thermal characterization by TG/DTG showed three well-defined thermal decomposition stages: dehydration; pyrolysis, carbonate decomposition. X-ray diffraction indicated the presence of an amorphous phase at 400°C and the increase of the relative crystallinity starting from 500°C, for the $Ca_xSr_{1-x}WO_4$ system studied. All the samples presented a tetragonal scheelite-type structure.

Acknowledgements

The authors thank the Brazilian agencies CAPES, FINEP and CNPq for financial support.

References

1 A. Kuzmin and J. Purans, Radiat. Meas., 33 (2001) 583.
2 A. A. Kaminskii, C. L. McCradius, H. R. Lee, D. A. Temple, T. H. Chyba, W. D. Marsh, J. C. Barnes, A. N. Annanenkov, V. D. Legun, H. J. Eichler, G. M. A. Gad and K. Ueda, Opt. Commun., 183 (2000) 277.
3 W. S. Cho and M. Yoshimura, J. Appl. Phys., 83 (1998) 518.
4 S. Saito, A. Kudo and T. Sakata, B. Chem. Soc. Jpn., 69 (1996) 1241.
5 F. R. C. Ciaco, F. M. Pontes, C. D. Pinheiro, E. R. Leite, R. S. Lazarro, J. A. Varela, C. A. Paskocimas, A. G. Souza and L. Elson, Cerâmica, 50 (2004) 43.
6 G. Blasse and W. J. Schipper, Phys. Status Solid A, 25 (1974) 173.
7 M. Pechini, US Patent No. 3,330,697, 1967.
8 C. S. Xavier, C. E. F. Costa, S. C. L. Crispim, M. I. B. Bernardi, M. A. M. A. Maurera, M. M. Conceition, E. Longo and A. G. Souza, J. Therm. Anal. Cal., 75 (2004) 461.
9 D. S. Gouveia, R. Rosenhaim, M. A. M. A. Maurera, S. J. G. Lima, C. A. Paskocimas, E. Longo, I. M. G. Santos and A. G. Souza, J. Therm. Anal. Cal., 75 (2004) 453.